



Agricultural drought disaster risk assessment in Shandong Province, China

Wentong Yang¹ · Liyuan Zhang¹ · Chunlei Liang¹

Received: 18 January 2022 / Accepted: 12 June 2023 / Published online: 26 June 2023
© The Author(s), under exclusive licence to Springer Nature B.V. 2023

Abstract

Shandong Province, the main grain-producing area in China, has ranked first in China in terms of total agricultural output value for many years. However, droughts with high frequency and long duration have been hindering local agricultural production. This paper aims to assess the risk of drought disasters in Shandong Province. Firstly, based on the natural disaster system theory, an agricultural drought disaster risk assessment model is developed. This model is applied to assess the agricultural drought hazard, exposure, vulnerability, emergency response and recovery capability, and agricultural drought disaster risk from 2012 to 2020. Secondly, risk uncertainty is analyzed through the evolution of risk over the past years. Finally, the accuracy of the risk assessment is verified through agricultural drought-related losses. The results show that: (1) The risk assessment results are in good agreement with the actual drought losses. (2) From the spatial scale, the high-risk areas of agricultural drought disasters were mainly located in the western part of Shandong Province. High-hazard areas of drought were located in eastern Shandong Province, and areas with high agricultural exposure and vulnerability were concentrated in the western part of the province, and the emergency response and recovery capacity of Rizhao and Zaozhuang was low. (3) From the time scale, there was high uncertainty of agricultural drought disaster risk in Dongying, Qingdao, and Heze in 2012–2020, all of which had reached a high-risk level of agricultural drought disaster several times. The agricultural exposure in Dongying, the agricultural vulnerability in Heze, and the emergency response and recovery capacity in Heze and Linyi all showed an increasing trend. The interannual variation characteristics and spatial zoning of agricultural drought risk are explored, and it is instructive for risk decision-makers to better develop drought response measures and improve drought resilience.

Keywords Drought disaster · Risk assessment · Risk uncertainty · Shandong province

✉ Liyuan Zhang
taianzlyls@163.com

¹ School of Management, Shandong University of Technology, Zibo 255049, China

1 Introduction

Drought is a phenomenon in which the precipitation is significantly less than the multi-year average precipitation during a certain period (Dracup et al. 1980). When the water supply is insufficient to meet the water needs of the population and causes economic losses and human casualties, which is called a drought disaster (Bi et al. 2021), drought disasters pose a serious threat to climate-sensitive economic sectors, especially the agricultural sector (Simelton et al. 2012; Liu et al. 2018). More than 7% of global crop output loss comes from drought (Lesk et al. 2016). In recent years, with the uneven spatiotemporal distribution of precipitation, changes in land surface factors, and human activities, drought disasters have occurred frequently in China (Zhang et al. 2020b). Shandong Province leads the rest of China in arable land rate, which has long ranked first in agricultural growth value. However, the drought disaster has been affecting local agricultural development (Wang et al. 2019). From the China Drought and Water Disaster Bulletin, the agricultural drought-affected area in Shandong Province reached 570,000 hectares in the past four years, of which 36,300 hectares were in extinction. Therefore, it is necessary to develop risk assessment work to promote regional drought planning and improve drought mitigation capacity. Furthermore, this facilitates emergency decision-making in disasters and thus reduces food losses (Zhang et al. 2022).

Drought disaster risk assessment can be divided into three main categories (Qu et al. 2018), i.e., the mathematical and statistical-based assessment method, the assessment method based on the physical formation mechanism, and the indicator system method. Historical disaster data contain the process of disaster evolution. The mathematical and statistical-based assessment method can be used to refine historical data to calculate trends of disaster evolution and risk probabilities (Sun et al. 2020). The method is limited by the availability of data information and requires a high length and accuracy of historical data, e.g., through the statistics of the main hydrological disaster data in Urumqi from 1949 to 2015; Li et al. (2019) identified and analyzed the risk characteristics and integrated distribution of hydrological disasters in the city. Bahrami et al. (2021) assessed the spatial and temporal distribution of drought severity in the Iranian region from 1967 to 2014 by using a standardized reconnaissance drought index (RDIst) and further assessed the trend by parametric and nonparametric statistical tests. By using the improved linkage number and entropy information diffusion method, Chen et al. (2020) assessed the risk of agricultural drought disasters in the Huabei Plain. The assessment method based on the physical formation mechanism can be used to describe the physical process of drought disaster formation. The internal linkages and evolutionary processes among the components of drought disaster risk can be obtained; however, this method requires high spatial resolution of the data and is complicated to operate. Zhu et al. (2021) used the AquaCrop model to simulate the yield of maize under different irrigation scenarios; furthermore, vulnerability curves (a function of DHI and yield loss rate) were developed for the entire growing season and each growth stage. Li et al. (2020) used the partial least squares regression method to analyze the effects of climate change and non-climatic factors on NDVI dynamics and drought risk, thus exploring the key drivers of risk formation. The indicator system method is the most commonly used in drought disaster risk assessment. The regional disaster system theory and natural disaster system theory are used to construct the indicator system. The regional disaster system theory can be used to divide disaster risk sources into disaster-formative factors, disaster-formative environment, disaster-affected bodies, and emergency response

and recovery capability (Yang et al. 2021). The natural disaster system theory can be used to divide disaster risk sources into hazard, exposure, vulnerability, and emergency response and recovery capability (Jia et al. 2016). Then we get specific indexes based on the source of risk, and the indicator weights are determined by the analytic hierarchy process (AHP) (Palchaudhuri and Biswas 2016), entropy weight method (Yi et al. 2018), CRITIC weight method (Krishnan et al. 2021), etc. And further, the index data are weighted to obtain the risk assessment value. Zarei et al. (2021) used the AHP and geographical information systems (GIS) to assess the sensitivity to the occurrence of different types of drought, such as meteorological drought, hydrological drought, and agricultural drought. Guo et al. (2021) assessed the degree of agricultural drought vulnerability in China by using the entropy weight method and the weighted composite score method; moreover, the contribution of the influencing factors was analyzed by the contribution model.

The previous indicators of drought hazard assessment include precipitation, temperature, evaporation, etc. However, these indicators do not provide a good description of the extent of drought hazards. Drought indices have been used to quantify drought, and a combination of drought indices and run theory (Yevjevich 1967) can be used to identify elements such as the duration, severity, and peak of the drought. Therefore, we use the drought index to assess the hazard level of drought. Drought indices can be generally categorized into drought indices based on ground climate data and remote sensing monitoring. The indices based on ground climate data are used to quantify the drought situation through statistical analysis of the observed data, e.g., the precipitation anomaly percentage (Zhao et al. 2019), the Palmer crop moisture index (CMI) (Ahamed et al. 2020), and the Standardized Runoff Indicator (SRI) (Shukla and Wood 2008), etc. Remote sensing has the advantages of high timeliness and wide coverage, which can realize the dynamic monitoring of drought. Drought indices based on remote sensing monitoring include the normalized difference vegetation index (NDVI) (Chu et al. 2019), the vegetation temperature condition index (VTCI) (Zhou et al. 2020), and the perpendicular drought index (PDI) (Nie et al. 2020), etc. The most common drought indices are the Palmer drought severity index (PDSI) (Wang et al. 2015; Yan et al. 2016), the standardized precipitation index (SPI) (Karimi et al. 2019; Bhunia et al. 2020), and the standardized precipitation evapotranspiration index (SPEI) (Zhang et al. 2020a; Musei et al. 2021). PDSI has been widely used as a more mature drought monitoring indicator, but the fixed time scale is its limitation. The SPI only considers the effect of precipitation on drought but ignores the effect of temperature on drought. Since SPEI compensates for the shortcomings of these two drought indices (Wang et al. 2017), we choose SPEI to assess the drought hazard level.

Currently, drought disaster risk assessments based on indicator systems are relatively mature (Dabanli 2018; Hoque et al. 2021), but most of them are assessed only for a particular year, and few studies have assessed the variation of drought disaster risk in inter-annual units. Due to the complexity of agricultural drought formation and the variability of the human social environment, the risk of agricultural drought disaster in each region varies significantly from year to year. Therefore, a risk assessment model is developed to evaluate agricultural drought disaster risk and to describe and assess the uncertainty of drought disaster risk over several years. Moreover, we count the changes in indicators in different regions in different years, which can reflect the sources of risk in different regions. Due to the consideration of data availability and timeliness, we validate the model based on meteorological, geographic, and social data of Shandong Province from 2012 to 2020. The output's results can provide quantitative direction for food security work.

2 Materials and methods

2.1 Study area

Shandong Province is a coastal province in East China (longitude $114^{\circ} 47.5' - 122^{\circ} 42.3'$ E and latitude $34^{\circ} 22.9' - 38^{\circ} 24.01' N$), which is 721.03 km long from east to west and 437.28 km long from north to south (Fig. 1). Shandong Province is a largely agricultural province (Xu et al. 2020). The province becomes the first province in China with a total agricultural output value of more than one trillion yuan in 2020, reaching 1019.06 billion yuan. However, the drought disaster has been hindering local agricultural development (Wang et al. 2019). The climate of Shandong Province is a warm-temperate monsoon climate, with low precipitation in spring and winter, and prone to drought disasters. With the increasing population and water demand, Shandong Province is more vulnerable to drought (Zuo et al. 2018). Therefore, it is instructive to develop an agricultural drought disaster risk assessment for Shandong Province to protect the local agricultural development.

2.2 Assessment indicators system and data sources

According to the four elements theory of natural disaster risk formation, natural disaster risk is composed of natural disaster hazard, exposure and vulnerability of the disaster-bearing body, and emergency response and recovery capability. According to this theory, the index system is shown in Table 1. Furthermore, food loss data from 2012 to 2020 are derived from the “China Water and Drought Disaster Bulletin” (The Ministry of Water Resources of the People’s Republic of China 2012–2020).

2.2.1 Hazard

(1) Annual drought conditions are described by the standardized precipitation evapotranspiration index on a 12-month time scale (SPEI-12) in December. SPEI (Vicente-Serrano et al. 2010) is an index to analyze the trend of drought evolution, which is

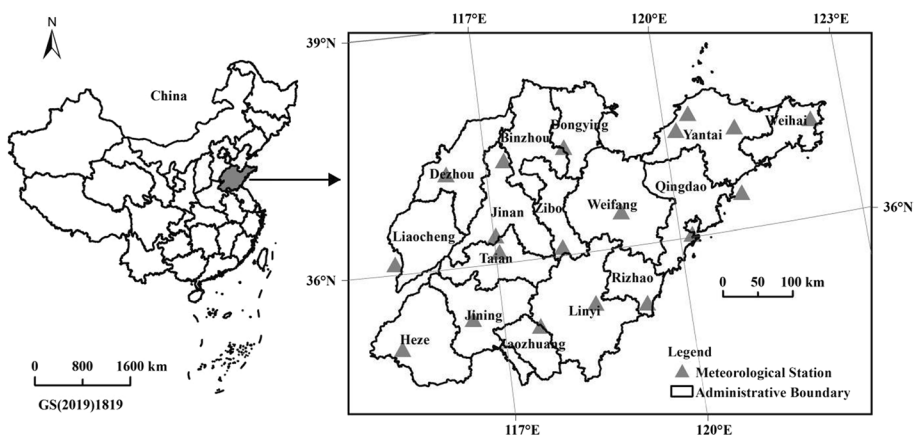


Fig. 1 Geographical location of the study area and meteorological stations

Table 1 Indicators system and data sources

| Factors | Indicator | Number | Correlation | Data sources |
|--|---|--------|-------------|---|
| Hazard | Dd | R_1 | + | Monthly meteorological data are derived from daily meteorological data of the China Meteorological Data Network (https://data.cma.cn) |
| | Ds | R_2 | - | |
| | Dp | R_3 | - | |
| | Annual drought conditions | R_4 | - | |
| | Annual normalized difference vegetation index | R_5 | - | |
| Exposure | Agricultural land (% of survey land) | E_1 | + | Modis data synthesized and downloaded by Google Earth Engine (https://earthengine.google.com) |
| | Grain crop sown area (% of the total sown area) | E_2 | + | |
| | Rural population (% of the total population) | E_3 | + | |
| Vulnerability | Use of agricultural plastic film (t/ha) | V_1 | - | Shandong Province Statistical Yearbook (Shandong Bureau of Statistics 2012–2020) |
| | Grain crops output (kg/ha) | V_2 | + | |
| | Grain output value per hectare (yuan/ha) | V_3 | + | |
| Emergency response and recovery capability | Disposable income of rural households (yuan/person) | B_1 | - | China Insurance Yearbook (China Banking and Insurance Regulatory Commission 2012–2020) |
| | Total power of agricultural machinery per hectare (kw/ha) | B_2 | - | |
| | Road density (km/ha) | B_3 | - | |
| | Agricultural insurance premiums (yuan) | B_4 | - | |

obtained by normal normalizing the cumulative probability distribution values of difference value series of precipitation and potential evapotranspiration. The calculation steps of SPEI are as follows:

Step 1: Calculate the potential evapotranspiration by the Thornthwaite method. After obtaining the temperature and latitude data of each meteorological station, we can calculate the potential evapotranspiration (PET).

$$PET = 16K \left(\frac{10T}{H} \right)^A, \tag{1}$$

$$H = \sum_{mon=1}^{12} \left(\frac{T_{mon,ave}}{5} \right)^{1.514}, \tag{2}$$

where K is the correction factor of a function of latitude and month, T represents the average monthly temperature, H represents the annual temperature efficiency index, and A represents a function of the heat index, $A = 6.75 \times 10^{-7}H^3 - 7.71 \times 10^{-5}H^2 + 1.79 \times 10^{-2}H + 0.492$.

Step 2: Get the difference values D_i between monthly precipitation and evapotranspiration.

$$D_i = P_i - PET_i, \tag{3}$$

where P_i is monthly precipitation, PET_i represents monthly evapotranspiration.

Step 3: Compute the SPEI series. The D series is fitted to the log-logistic probability distribution and then it was normalized, thus obtaining the SPEI series.

$$f(x) = \frac{\beta}{\alpha} \left(\frac{x-y}{\alpha} \right) \left[1 + \left(\frac{x-y}{\alpha} \right) \right]^{-2}, \tag{4}$$

where α , β , and γ are scale, shape, and origin parameters, respectively. The parameters α , β , and γ can be obtained by the linear moment (L-moment) method.

The probability distribution function of D is given in Eq. (5).

$$F(x) = \left[1 + \left(\frac{\alpha}{x-\gamma} \right) \right]^{-1}, \tag{5}$$

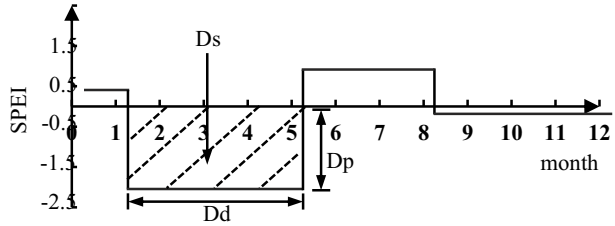
Step 4: Obtain the SPEI value. P is the probability that a given D value will be exceeded, $P = 1 - F(x)$. If $P \leq 0.5$, then $W = \sqrt{-2 \ln(P)}$; otherwise $W = \sqrt{-2 \ln(1 - P)}$, multiply the resulting SPEI value by -1 .

$$SPEI = W - \frac{C_0 + C_1W + C_2W^2}{1 + d_1W + d_2W^2 + d_3W^3}, \tag{6}$$

where $C_0=2.515517$, $C_1=0.802853$, $C_2=0.010328$, $d_1=1.432788$, $d_2=0.189269$, and $d_3=0.001308$.

(2) D_d , D_s , and D_p . Run theory can be used to identify drought events (Yevjevich 1967), and a drought event includes drought duration, drought severity, and drought peak (Fig. 2). Set the drought threshold as -0.5 , i.e., when the SPEI value is less than -0.5 , the month is in drought. $D_{d,i}$, the cumulative duration of all drought events in year i , is the count of months with SPEI values less than -0.5 in year i . $D_{s,i}$, the cumulative

Fig. 2 Schematic diagram showing the run theory



severity of all drought events in year i , is the sum of the SPEI values less than -0.5 in year i . Dp_i , the peak value of a drought event, is the minimum SPEI value in the year i .

(3) Annual normalized difference vegetation index is described by the average of the normalized difference vegetation index (NDVI) for each month of the year. NDVI is a commonly used drought index calculated based on remote sensing data and can be used to characterize the degree of drought (Chu et al. 2019; Liu et al. 2020). The index is calculated by near-infrared band reflectance and red band reflectance, which can reflect the sparsity of vegetation. In areas with little or no vegetation, the contrast between the two bands is small; in areas with dense vegetation, the contrast between the two bands is large.

$$NDVI = \frac{\rho_n - \rho_r}{\rho_n + \rho_r}, \tag{7}$$

where ρ_n is the near-infrared band reflectance and ρ_r is the red light band reflectance.

2.2.2 Agriculture exposure

Exposure of the disaster-bearing body indicates the number or value of disaster-bearing bodies exposed to the drought disaster, and the disaster-bearing body studied in this paper is agriculture. Both agricultural land (% of survey land) and grain crop sown area (% of the total sown area) are positive indicators (Zeng et al. 2019), i.e., the larger the proportion, the bigger the exposure to agriculture. Likewise, the rural population (% of the total population) is a positive indicator.

2.2.3 Agriculture vulnerability

The vulnerability of the disaster-bearing body indicates the extent of crop damage caused by drought disasters in a given region, and it synthetically reflects the extent of drought disaster damage. Agricultural films play an important role in moisturizing and insulating crops during the planting period, and it can effectively reduce the impact of drought on crops. The larger the grain crops output per hectare, the higher the grain output value per hectare, and the greater the potential loss (Luo et al. 2020).

2.2.4 Emergency response and recovery capability

Emergency response and recovery capability indicate the extent that the affected area recovers from the disaster in the long or short term. The total power of agricultural machinery per hectare determines the level of agricultural mechanization in the region, which determines the level of agricultural development. Therefore, the higher the total power of agricultural

machinery per hectare, the higher the level of agricultural development, and the greater the resistance to adversity (Liu et al. 2019). Disposable income of rural households and agricultural insurance premiums can effectively reduce the risk of drought disasters, both of which are negative indicators (Hagenlocher et al. 2019). The greater the density of the road network, the more conducive to doing disaster relief work in the event of a disaster (Duan et al. 2021).

2.3 The indicator system method

The calculation steps of the indicator system method are as follows: (1) standardization of indicator data. To eliminate the influence of different physical dimensions on decision-making, we standardize the positive indicator data with Eq. (8) and standardize the negative indicator data with Eq. (9).

$$A_{ij} = \frac{X_{ij} - \min \{X_{1j}, \dots, X_{nj}\}}{\max \{X_{1j}, \dots, X_{nj}\} - \min \{X_{1j}, \dots, X_{nj}\}}, \quad (8)$$

$$A_{ij} = \frac{\max \{X_{1j}, \dots, X_{nj}\} - X_{ij}}{\max \{X_{1j}, \dots, X_{nj}\} - \min \{X_{1j}, \dots, X_{nj}\}}, \quad (9)$$

where X_{ij} is the value corresponding to the j th indicator of the i th region. A_{ij} represents the standardized value of the j th indicator of the i th region.

(2) Calculate indicator weights. The AHP-entropy weight method is a common method for calculating indicator weights, and the indicator weights calculated by this method are more accurate (Sahana et al. 2021). The calculation steps are as follows:

Step 1: Calculate objective weights. The principle of the entropy weight method is that the smaller the information entropy of the indicator, the greater the variability of the indicator value, the more information the indicator provides, and thus the greater the weight of the indicator (Yi et al. 2018). The calculation steps can be divided into three parts: Firstly, normalize the indicator data; secondly, get the information entropy of each indicator; finally, determine the objective weights W_j^+ of each indicator.

Step 2: The subjective weights of the indicators are calculated by the AHP method (Palchaudhuri and Biswas 2016). The calculation steps can be divided into three parts: Firstly, the judgment matrix is constructed; secondly, the consistency test is performed; and finally, the weight vector of indicators is normalized to obtain the final weights W_j^- .

Step 3: The comprehensive indicator weight W_j is computed by Eq. (10).

$$W_j = \frac{W_j^+ \times W_j^-}{\sum_{j=1}^n W_j^+ \times W_j^-} \quad j = 1, \dots, n \quad (10)$$

where W_j^+ represents objective weight and W_j^- represents subjective weight.

(3) Calculate the assessment value. With the indicator weights obtained, we use the WAA algorithm (Merigo 2011) to calculate agricultural drought disaster risk assessment values.

$$WAA(Y) = y_{i1}W_1 + y_{i2}W_2 + \dots + y_{ij}W_j, \quad (11)$$

where y_{ij} represents the standardized value of the j th indicator for the i th region and W_j represents the weight value of each assessment indicator.

(4) Based on the average assessed values from 2012 to 2020, the natural breakpoint method is used to determine the different level ranges.

(5) ArcGIS software is used to visualize data. The multi-year mean of the indicator describes the perennial state of the risk, and the variance of the change in risk level over multiple years describes the degree of uncertainty of the risk.

2.4 The method of comprehensive percentage of production loss

The method of comprehensive percentage of production loss was derived from the “Drought Assessment Criteria,” which was issued by the Office of State Flood Control and Drought Relief Headquarters in China (Yang et al. 2022). C is agricultural drought disaster assessment values(%). The larger its value, the more severe the drought disaster loss.

$$C = I3 \times 90\% + (I2 - I3) \times 55\% + (I1 - I2) \times 20\%, \quad (12)$$

where $I1$ is the affected area (more than 10% yield reductions) as a percentage of the sown area, $I2$ represents the damaged area (more than 30% yield reductions) as a percentage of the sown area, and $I3$ represents the extinction area (more than 80% yield reductions) as a percentage of the sown area.

3 Results and discussion

3.1 Agricultural drought disaster risk assessment in Shandong Province

Based on the indicator system method to assess the risk of agricultural drought disasters in Shandong Province, the subjective weights calculated by AHP, the objective weights calculated by the entropy weight method, and the combined weights calculated by Eq. (1) are all shown in Table 2.

Based on the average assessed values from 2012 to 2020, the natural breakpoint method is used to determine the different agricultural drought disaster risk level ranges, i.e., low (0–0.4196), lower (0.4197–0.4742), moderate (0.4743–0.4923), higher (0.4924–0.5145), and high (0.5146–1). ArcGIS software is used to visualize data. The multi-year mean of the indicator describes the perennial state of the risk, and the variance of the change in risk level over multiple years describes the degree of uncertainty of the risk.

The distribution of agricultural drought disaster risk and risk uncertainty in Shandong Province from 2012 to 2020 (Fig. 3) is as follows: (1) High-risk areas for agricultural drought disasters were frequently located in the western part of Shandong Province. Moreover, the overall agricultural drought disaster risk in Shandong Province was higher in 2014, 2019, and 2020 and lower in 2015 and 2016. (2) The risk uncertainty in Liaocheng and Zaozhuang was low, and both regions had been at high risk of agricultural drought disasters from 2012 to 2020, so attention should be paid to the prevention of drought disasters in the two regions. Agricultural drought disaster risk in Weihai City is consistently at a low level from 2012 to 2020. (3) There was a high degree of uncertainty in agricultural drought disaster risk in Dongying, Qingdao, and Heze. The agricultural drought disasters in Dongying were at a high-risk level in 2014, 2017, 2019, and 2020, Qingdao was at a high-risk level in 2015 and 2019, and Heze was at a high-risk level in 2012, 2013, and 2020. (4) High-risk areas for agricultural drought disasters in 2012–2020 were located in

Table 2 Indicator weights

| Indicator number | R_1 | R_2 | R_3 | R_4 | R_5 | E_1 | E_2 | E_3 | V_1 | V_2 | V_3 | B_1 | B_2 | B_3 | B_4 |
|------------------|--------|--------|--------|--------|--------|--------|--------|--------|--------|--------|--------|--------|--------|--------|--------|
| W_j^+ | 0.0949 | 0.0949 | 0.0721 | 0.0411 | 0.0756 | 0.0293 | 0.0795 | 0.0702 | 0.0272 | 0.0633 | 0.098 | 0.0733 | 0.0293 | 0.082 | 0.0693 |
| W_j^- | 0.0522 | 0.0609 | 0.0348 | 0.0696 | 0.0869 | 0.0725 | 0.0906 | 0.0543 | 0.0626 | 0.0939 | 0.1043 | 0.0593 | 0.0527 | 0.0395 | 0.0659 |
| W_j | 0.0735 | 0.0858 | 0.0372 | 0.0425 | 0.0975 | 0.0315 | 0.1069 | 0.0566 | 0.0253 | 0.0882 | 0.1517 | 0.0645 | 0.0229 | 0.0481 | 0.0678 |

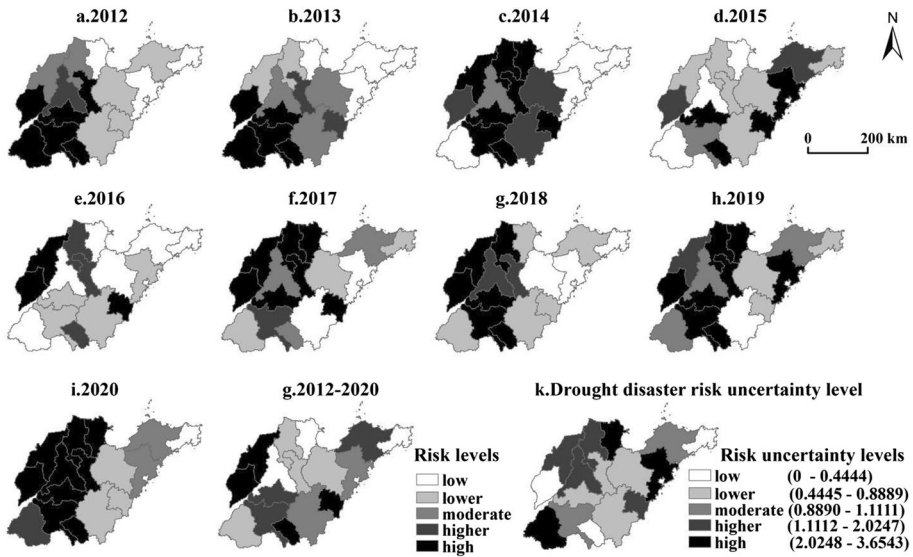


Fig.3 Map of drought disaster risk and risk uncertainty in Shandong Province, 2012–2020

Dezhou, Liaocheng, Zaozhuang, and Rizhao, and it is important to focus on drought mitigation in these areas.

3.2 Risk causes of agricultural drought disasters in Shandong Province

3.2.1 Drought hazard analysis in Shandong Province

Based on the indicator system method to assess the drought hazard in Shandong Province. The five drought hazard indicators in Table 1 and the corresponding indicator weights in Table 2 are used to assess the drought hazard of different regions, i.e., $W_{R_1} = 0.0735$, $W_{R_2} = 0.0858$, $W_{R_3} = 0.0372$, $W_{R_4} = 0.0425$, and $W_{R_5} = 0.0975$. Based on the average assessed values from 2012 to 2020, the natural breakpoint method is used to determine the different drought hazard level ranges, i.e., low (0–0.0812), lower (0.0813–0.1066), moderate (0.1067–0.1299), higher (0.1300–0.2175), and high (0.2176–1).

The distribution of drought hazard and hazard uncertainty in Shandong Province from 2012 to 2020 (Fig. 4) is as follows: (1) High-hazard areas of drought are frequently concentrated in the eastern part of Shandong Province. Moreover, the overall drought hazard in Shandong Province is higher in 2018 and 2020 and lower in 2015 and 2016. (2) The uncertainty level of drought hazard in Yantai, Weifang, Zibo, Linyi, and Rizhao is low. Among them, the drought hazard is higher in Yantai, Weifang, Linyi, and Rizhao, and lower in Zibo. (3) The degree of uncertainty of drought hazard is high in Weihai, Dezhou, and Heze cities. The drought hazard is higher in Weihai City in 2015, 2017, 2019, and 2020, Dezhou City in 2014, 2017, 2018, and 2020, and Heze City in 2012 and 2013. (4) The high-hazard areas of drought in 2012–2020 are located in Yantai, Qingdao, and Rizhao, which can reduce the risk of agricultural drought disasters by strengthening disaster monitoring and early warning.

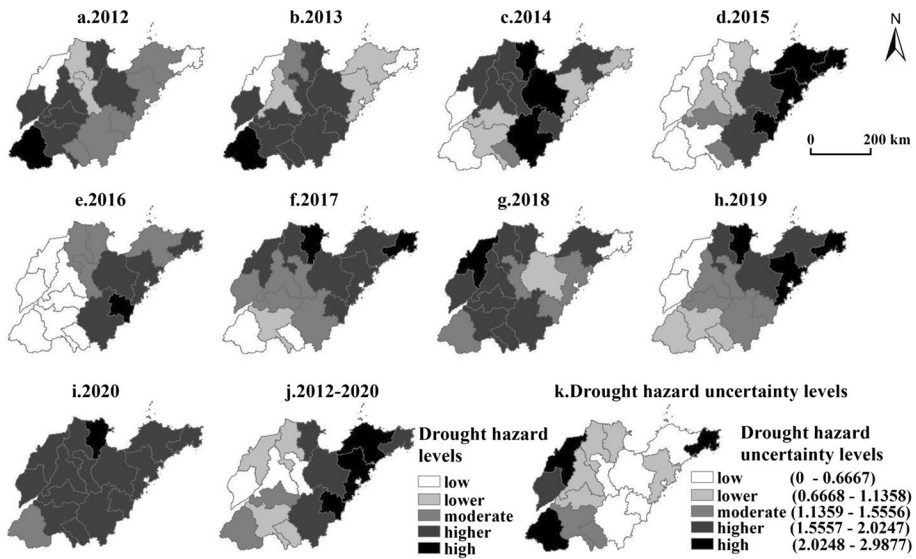


Fig. 4 Map of drought hazard and hazard uncertainty in Shandong Province, 2012–2020

3.2.2 Agricultural exposure analysis in Shandong Province

Based on the indicator system method to assess the agricultural exposure in Shandong Province, the three agricultural exposure indicators in Table 1 and the corresponding indicator weights in Table 2 are used to assess the agricultural exposure of different regions, i.e., $W_{E_1}=0.0315$, $W_{E_2}=0.1069$, and $W_{E_3}=0.0566$. Based on the average assessed values from 2012 to 2020, the natural breakpoint method is used to determine the agricultural exposure level ranges, i.e., low (0–0.0419), lower (0.0420–0.0843), moderate (0.0844–0.0979), higher (0.0980–0.1382), and high (0.1383–1).

The distribution of agricultural exposure and agricultural exposure uncertainty in Shandong Province from 2012 to 2020 (Fig. 5) is as follows: (1) The areas with high agricultural exposure are mainly concentrated in the western part of Shandong Province, and the changes over multiple years are minor. (2) The uncertainty level of agricultural exposure was lower in Dezhou, Liaocheng, Zibo, Jining, and Heze, which are areas with higher agricultural exposure. (3) The uncertainty level of agricultural exposure in Dongying is high, and the degree of agricultural exposure in the area shows an increasing trend. (4) The high agricultural exposure areas in 2012–2020 are located in Dezhou and Liaocheng cities, where agricultural drought resistance can be enhanced through the development of digital, water-saving agriculture.

3.2.3 Agricultural vulnerability analysis in Shandong Province

Based on the indicator system method to assess the agricultural vulnerability in Shandong Province, the three agricultural vulnerability indicators in Table 1 and the corresponding indicator weights in Table 2 are used to assess the agricultural vulnerability of different regions, i.e., $W_{V_1}=0.0253$, $W_{V_2}=0.0882$, and $W_{V_3}=0.1517$. Based on the average assessed

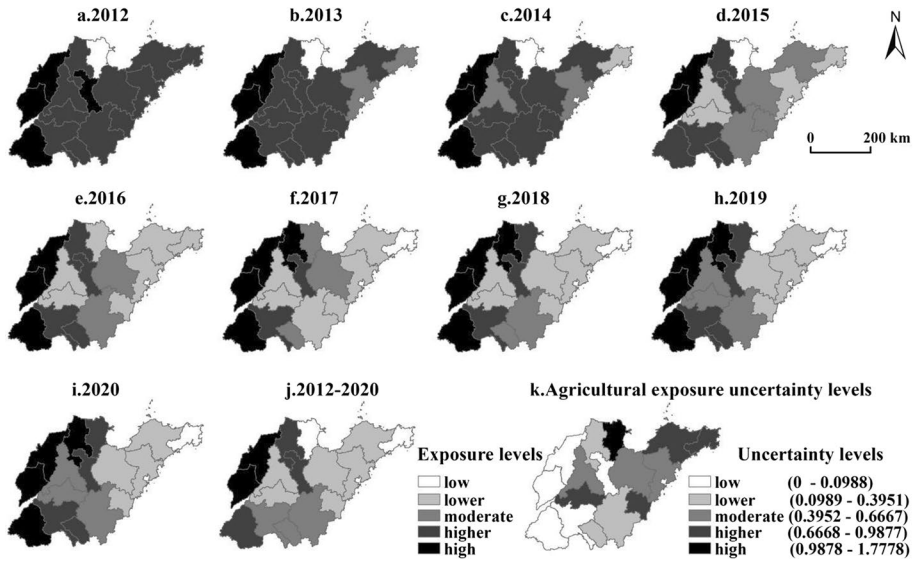


Fig. 5 Map of agricultural exposure and exposure uncertainty in Shandong Province, 2012–2020

values from 2012 to 2020, the natural breakpoint method is used to determine the agricultural vulnerability level ranges, i.e., low (0–0.0359), lower (0.0360–0.0935), moderate (0.0936–0.1333), higher (0.1334–0.1893), and high (0.1894–1).

The distribution of agricultural vulnerability and agricultural vulnerability uncertainty in Shandong Province from 2012 to 2020 (Fig. 6) is as follows: (1) Areas of high agricultural vulnerability are concentrated in the western part of Shandong Province, and there has been slight change over multiple years. (2) The uncertainty level of agricultural vulnerability is lower in Dezhou, Binzhou, and Jining, which are areas with higher agricultural vulnerability. (3) The uncertainty level of agricultural vulnerability in Heze is high, and the degree of agricultural vulnerability in the area shows an increasing trend. (4) The high agricultural vulnerability area in 2012–2020 is located in Jining City, where losses can be reduced by promoting agricultural insurance and improving the disaster response platform.

3.2.4 Emergency response and recovery capability in Shandong Province

Based on the indicator system method to assess the emergency response and recovery capability in Shandong Province, the four emergency response and recovery capability indicators in Table 1 and the corresponding indicator weights in Table 2 are used to assess the emergency response and recovery capability of different regions, i.e., $W_{B_1} = 0.0645$, $W_{B_2} = 0.0229$, $W_{B_3} = 0.0481$, and $W_{B_4} = 0.0678$. Based on the average assessed values from 2012 to 2020, the natural breakpoint method is used to determine the emergency response and recovery level ranges, i.e., low (0–0.0424), lower (0.0425–0.0779), moderate (0.0780–0.0935), higher (0.0936–0.1188), and high (0.1189–1).

The distribution of emergency response and recovery capability and capability uncertainty in Shandong Province from 2012 to 2020 (Fig. 7) is as follows: (1) The high emergency response and recovery capability areas from 2012 to 2020 are mainly concentrated

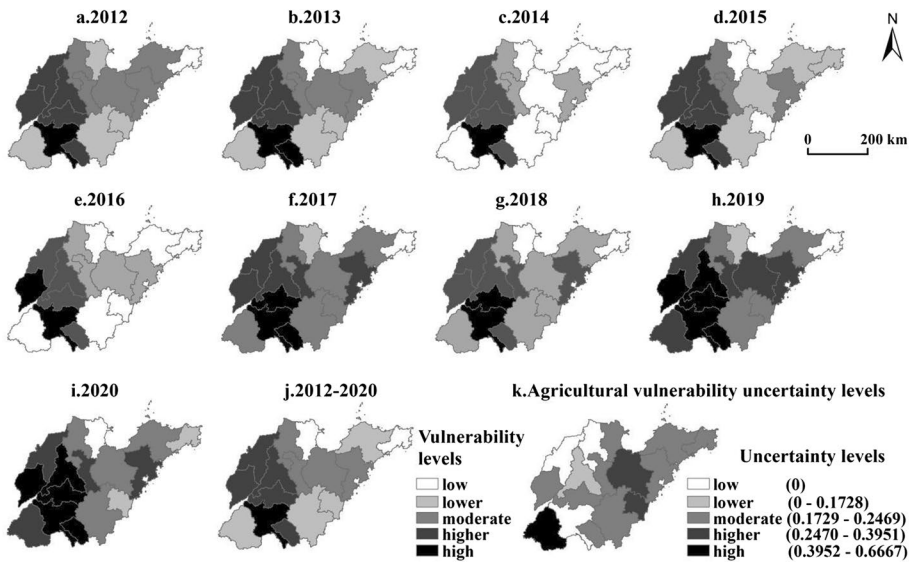


Fig. 6 Map of agricultural vulnerability and vulnerability uncertainty in Shandong Province, 2012–2020

in Weifang, Qingdao, and Dezhou, and the low capability areas are mainly concentrated in Rizhao and Zaozhuang. (2) There is a low level of uncertainty in the emergency response and recovery capabilities of Dongying, Weifang, and Yantai cities. Among them, the emergency response and recovery capabilities of Weifang and Yantai are consistently strong, while those of Dongying is consistently weak. (3) The uncertainty levels of emergency

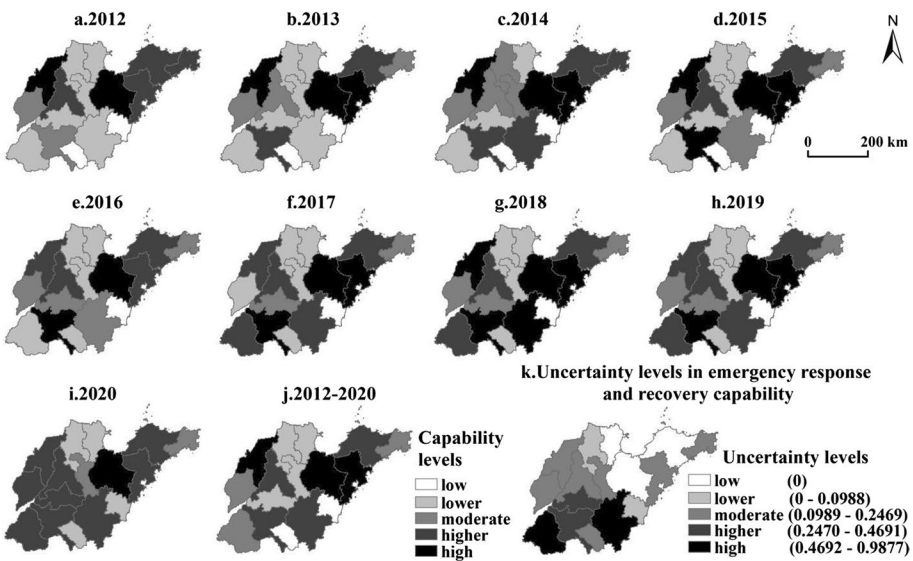


Fig. 7 Map of emergency response and recovery capability and capability uncertainty in Shandong Province, 2017–2020

response and recovery capabilities in Heze and Linyi are high, and the capabilities in both areas show an increasing trend.

3.3 Discussion

3.3.1 The Rationality of the constructed model

(1) The rationality of the indicator system. The SPEI based on the Thornthwaite method can be used for quantitative analysis of drought in Shandong (Zuo et al. 2018; Yao et al. 2021; Yang et al. 2023). Moreover, SPEI-3 can be used to assess agricultural drought conditions in Shandong (Zuo et al. 2018), and it is reasonable to identify the duration (Dd), severity (Ds), and peak (Dp) of agricultural drought based on SPEI-3. Also, it has been documented that NDVI can be used to quantify the drought status in Shandong Province (Liu et al. 2020).

Other indicators are appropriate for assessing agricultural drought disaster risk, i.e., Agricultural land (% of survey land) (Zeng et al. 2019), grain crop sown area (% of the total sown area) (Zeng et al. 2019), the rural population (% of the total population) (Palchaudhuri et al. 2016), Agricultural films (Zhang et al. 2019), the grain crops output per hectare (Luo et al. 2020), the grain output value per hectare, (Luo et al. 2020), the total power of agricultural machinery (Liu et al. 2019), disposable income of rural households (Hagenlocher et al. 2019), agricultural insurance premiums (Hagenlocher et al. 2019), and the density of the road network (Duan et al. 2021).

(2) To further verify the ability of this paper to assess drought disaster risk, we compared the drought disaster risk distribution and drought disaster loss derived from each year's assessment. The moderate and above level of risk can cause significant losses, and we counted the number of cities with moderate and above levels from 2012 to 2020. At the same time, we calculate the year-by-year drought loss values by using the method of comprehensive percentage of production loss (Fig. 8). By comparing them, we find that the trends are almost the same. Based on the relationship between high risk and high loss, it shows that the assessment results of this paper are reasonable.

3.3.2 Risk causes in high-risk areas

This paper presents a detailed analysis of the overall components of agricultural drought disaster risk in Shandong Province. By calculating the drought hazard, agricultural exposure and vulnerability, emergency response and recovery capacity, and comprehensive risk in 2012–2020, the distribution of agricultural drought disaster risk and risk development

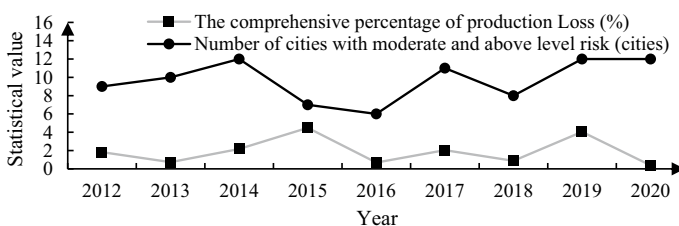


Fig. 8 Drought disaster risk and drought disaster losses

trends of Shandong Province in different years in recent years can be obtained. Moreover, the average of the last nine years is calculated to reflect the perennial risk status of different regions, and the variance of level change is used to describe the risk uncertainty of different regions. With the above information, it is convenient for risk decision-makers to find out the shortcomings of the drought work in each city and propose corresponding drought strategies.

Through the four risk causes analysis, we can grasp the causes of high risk of agricultural drought disasters in Dezhou, Liaocheng, Zaozhuang, and Rizhao cities. (1) The causes of the high risk of agricultural drought disasters in Dezhou are mainly high agricultural exposure and high agricultural vulnerability. The city has the highest grain crop sown area (% of the total sown area) at 0.86%, which is the reason for the high agricultural exposure. The city has the highest grain yield per hectare at 7319 kg/ha, which explains the high agricultural vulnerability of the area. (2) The high agricultural exposure and vulnerability of Liaocheng City lead to a high risk of agricultural drought disasters in the area. The city has the most agricultural land (% of survey land) at 0.8%, which explains the high agricultural exposure in the area. And the high grain yield and production value per hectare of agricultural land in the city, 6705 kg/ha and 56,000 yuan/ha, are the reasons for the high agricultural vulnerability in the area. (3) The causes of the high risk of agricultural drought disasters in Zaozhuang City are high agricultural vulnerability and weak emergency response and recovery capability. The city has a high grain production value per hectare of 57,700 yuan/ha, which results in high agricultural vulnerability in the area. The total power of agricultural machinery per hectare is the lowest in the area, about 8.11kw/ha, which is the reason for the weak emergency response and recovery capability. (4) The causes of the high risk of agricultural drought disaster in Rizhao are high drought hazard and weak emergency response and recovery capability. The city has the longest annual drought duration, averaging 4.33 months, and the highest drought intensity, averaging 4.51 units, which explains the high hazard of drought in the area. The lowest agricultural insurance premium in the city was 43.53 million yuan, which explains the weak emergency response and recovery capability.

4 Conclusion

Based on meteorological, geographical, and social data of Shandong Province from 2012 to 2020, the risk of agricultural drought disasters in Shandong Province and the degree of risk uncertainty are assessed. Moreover, the risk causation analysis is conducted in four aspects of drought hazards, agricultural exposure, agricultural vulnerability, and emergency response and recovery capacity. The findings of the study are as follows:

From the spatial scale, (1) the high-risk areas of agricultural drought disasters were mainly located in the western part of Shandong Province. Moreover, it was mainly concentrated in Dezhou, Liaocheng, Zaozhuang, and Rizhao, and it is important to focus on the drought mitigation work in these areas. (2) The high-hazard areas of drought were mainly located in the eastern part of Shandong Province, mainly in Yantai, Qingdao, and Rizhao cities. (3) Areas with high agricultural exposure were concentrated in the western part of Shandong Province, mainly in Dezhou and Liaocheng. (4) Areas with high agricultural vulnerability were concentrated in the western part of Shandong Province, mainly in Jining City. (5) The areas with low emergency response and recovery capacity were mainly concentrated in Rizhao and Zaozhuang.

From the temporal scale, (1) agricultural drought disaster risk in Shandong Province was high in 2014, 2019, and 2020. Furthermore, there was a high uncertainty of agricultural drought disaster risk in Dongying, Qingdao, and Heze in 2012–2020, all of which had reached a high-risk level of agricultural drought disaster several times. (2) The overall drought hazard in Shandong Province was higher in 2018 and 2020, and the uncertainty level of drought hazard was high in Weihai, Dezhou, and Heze cities. (3) There was little change in agricultural exposure in Shandong Province from 2012 to 2020. Among them, the uncertainty level of the agricultural risk exposure was higher in Dongying, and the agricultural risk exposure in this region showed an increasing trend. (4) There had been a slight change in agricultural vulnerability in Shandong Province over the years. And the uncertainty level of agricultural vulnerability in Heze was high, and the degree of agricultural vulnerability in the region was on the rise. (5) The uncertainty of emergency response and recovery capacity in Heze and Linyi was high, and the capacity in both places was on the rise.

Acknowledgements This work was supported by the National Social Science Foundation of China (19CGL045).

Authors contribution WY contributed to conceptualization, methodology, modeling, and writing—original draft. LZ contributed to funding acquisition, supervision, and writing—review and editing. CL contributed to validation, and writing—review and editing.

Funding The National Social Science Foundation of China (19CGL045).

Declarations

Competing interest The authors declare that they have no known competing financial interests or personal relationships that could have appeared to influence the work reported in this paper.

References

- Ahamed S, Homs R, Khan N, Shahid S, Shiru M, Mohsenipour M, Ahmed K, Nawaz N, Alias N, Yuzir A (2020) Assessment of changing pattern of crop water stress in Bangladesh. *Environ Dev Sustain* 22:4619–4637. <https://doi.org/10.1007/s10668-019-00400-w>
- Bahrami M, Bazrkar S, Zarei A (2021) Spatiotemporal investigation of drought pattern in Iran via statistical analysis and GIS technique. *Theor Appl Climatol* 143:1113–1128. <https://doi.org/10.1007/s00704-020-03480-1>
- Bhunia P, Das P, Maiti R (2020) Meteorological drought study through spi in three drought prone districts of west Bengal, India. *Earth Syst Environ* 4:43–55. <https://doi.org/10.1007/s41748-019-00137-6>
- Bi S, Qiu X, Wang G, Gong Y, Wang L, Xu M (2021) Spatial distribution characteristics of drought disasters in Hunan province of China from 1644 to 1911 based on EOF and REOF methods. *Environ Earth Sci* 80:1–11. <https://doi.org/10.1007/s12665-021-09867-1>
- Chen M, Ning S, Jin J, Cui Y, Wu C, Zhou Y (2020) Risk assessment of agricultural drought disaster on the Huaibei plain of China based on the improved connection number and entropy information diffusion method. *Water-Sui* 12:1089. <https://doi.org/10.3390/w12041089>
- China Banking and Insurance Regulatory Commission (2012–2020) Yearbook of China's Insurance 2013–2021. China Insurance Yearbook Club, Beijing (in Chinese)
- Chu H, Venevsky S, Wu C, Wang M (2019) NDVI-based vegetation dynamics and its response to climate changes at amur-Heilongjiang river basin from 1982 to 2015. *Sci Total Environ* 650:2051–2062. <https://doi.org/10.1016/j.scitotenv.2018.09.115>
- Dabanli I (2018) Drought hazard, vulnerability, and risk assessment in turkey. *Arab J Geosci* 11:1–12. <https://doi.org/10.1007/s12517-018-3867-x>
- Dracup J, Lee K, Paulson E (1980) On the definition of droughts. *Water Resour Manag* 16:297–302. <https://doi.org/10.1029/WR016i002p00297>

- Duan Y, Xiong J, Cheng W, Wang N, Li Y, He Y, Liu J, He W, Yang G (2021) Flood vulnerability assessment using the triangular fuzzy number-based analytic hierarchy process and support vector machine model for the belt and road region. *Nat Hazards*. <https://doi.org/10.1007/s11069-021-04946-9>
- Guo H, Chen J, Pan C (2021) Assessment on agricultural drought vulnerability and spatial heterogeneity study in China. *Int J Env Res Pub He* 18:4449. <https://doi.org/10.3390/ijerph18094449>
- Hagenlocher M, Meza I, Anderson C, Min A, Renaud F, Walz Y, Siebert S, Sebesvari Z (2019) Drought vulnerability and risk assessments: state of the art, persistent gaps, and research agenda. *Environ Res Lett* 14:083002. <https://doi.org/10.1088/1748-9326/ab225d>
- Hoque M, Pradhan B, Ahmed N, Sohel M (2021) Agricultural drought risk assessment of northern new south Wales, Australia using geospatial techniques. *Sci Total Environ* 756:143600. <https://doi.org/10.1016/j.scitotenv.2020.143600>
- Jia J, Han L, Liu Y, He N, Zhang Q, Wan X, Zhang Y, Hu J (2016) Drought risk analysis of maize under climate change based on natural disaster system theory in southwest China. *Acta Ecol Sin* 36:340–349. <https://doi.org/10.1016/j.chnaes.2016.06.001>
- Karimi M, Melesse A, Khosravi K, Mamuye M, Zhang J (2019) Analysis and prediction of meteorological drought using SPI index and Arima model in the Karkheh river basin, Iran. In: *Extreme hydrology and climate variability*. Elsevier, pp 343–353. <https://doi.org/10.1016/B978-0-12-815998-9.00026-9>
- Krishnan A, Kasim M, Hamid R, Ghazali M (2021) A modified critic method to estimate the objective weights of decision criteria. *Symmetry* 13:973. <https://doi.org/10.3390/sym13060973>
- Lesk C, Rowhani P, Ramankutty N (2016) Influence of extreme weather disasters on global crop production. *Nature* 529:84–87. <https://doi.org/10.1038/nature16467>
- Li X, Du J, Long H, Sun G (2019) Characteristics and risk analysis of hydrological disaster events from 1949 to 2015 in Urumqi, China. *Theor Appl Climatol* 137:745–754. <https://doi.org/10.1007/s00704-018-2630-2>
- Li K, Tong Z, Liu X, Zhang J, Tong S (2020) Quantitative assessment and driving force analysis of vegetation drought risk to climate change: methodology and application in northeast China. *Agric For Meteorol* 282:107865. <https://doi.org/10.1016/j.agrformet.2019.107865>
- Liu X, Pan Y, Zhu X, Yang T, Bai J, Sun Z (2018) Drought evolution and its impact on the crop yield in the north China plain. *J Hydrol* 564:984–996. <https://doi.org/10.1016/j.jhydrol.2018.07.077>
- Liu Y, You M, Zhu J, Wang F, Ran R (2019) Integrated risk assessment for agricultural drought and flood disasters based on entropy information diffusion theory in the middle and lower reaches of the Yangtze River, China. *Int J Disast Risk Reduct* 38:101. <https://doi.org/10.1016/j.ijdr.2019.101194>
- Liu Q, Zhang S, Zhang H, Bai Y, Zhang J (2020) Monitoring drought using composite drought indices based on remote sensing. *Sci Total Environ* 711:134585. <https://doi.org/10.1016/j.scitotenv.2019.134585>
- Luo D, Ye L, Sun D (2020) Risk evaluation of agricultural drought disaster using a grey cloud clustering model in Henan Province, China. *Int J Disast Risk Reduct* 49:101759. <https://doi.org/10.1016/j.ijdr.2020.101759>
- Merigo J (2011) A unified model between the weighted average and the induced OWA operator. *Expert Syst Appl* 38(9):11560–11572. <https://doi.org/10.1016/j.eswa.2011.03.034>
- Musei S, Nyaga J, Dubow A (2021) Spei-based spatial and temporal evaluation of drought in Somalia. *J Arid Environ* 184:104296. <https://doi.org/10.1016/j.jaridenv.2020.104296>
- Nie Y, Tan Y, Deng Y, Yu J (2020) Suitability evaluation of typical drought index in soil moisture retrieval and monitoring based on optical images. *Remote Sens Basel* 12:2587. <https://doi.org/10.3390/rs12162587>
- Palchadhuri M, Biswas S (2016) Application of AHP with GIS in drought risk assessment for Puruliya district, India. *Nat Hazards* 84:1905–1920. <https://doi.org/10.1007/s11069-016-2526-3>
- Qu Y, Lv J, Su Z, Sun H, Ma M (2018) Research review and perspective of drought mitigation. *J Hydraul Eng* 49:115–125 (in Chinese)
- Sahana V, Mondal A, Sreekumar P (2021) Drought vulnerability and risk assessment in India: sensitivity analysis and comparison of aggregation techniques. *J Environ Manage* 299:113689. <https://doi.org/10.1016/j.jenvman.2021.113689>
- Shandong Bureau of Statistics (2012–2020) *Shandong Statistical Yearbook 2013–2021*. China Statistics Press, Beijing (in Chinese)
- Shukla S, Wood A (2008) Use of a standardized runoff index for characterizing hydrologic drought. *Geophys Res Lett*. <https://doi.org/10.1029/2007GL032487>
- Simelton E, Fraser E, Termansen M, Benton T, Gosling S, South A, Arnell N, Challinor A, Dougill A, Forster P (2012) The socioeconomics of food crop production and climate change vulnerability: a global scale quantitative analysis of how grain crops are sensitive to drought. *Food Secur* 4:163–179. <https://doi.org/10.1007/s12571-012-0173-4>

- Sun R, Gao G, Gong Z, Wu J (2020) A review of risk analysis methods for natural disasters. *Nat Hazards* 100:571–593. <https://doi.org/10.1007/s11069-019-03826-7>
- The Ministry of Water Resources of the People's Republic of China (2012–2020) China Water and Drought Disaster Bulletin. China Cartographic Publishing House, Beijing (in Chinese)
- Vicente-Serrano S, Begueria S, López-Moreno J (2010) A multiscale drought index sensitive to global warming: the standardized precipitation evapotranspiration index. *J Clim* 23:1696–1718. <https://doi.org/10.1175/2009JCLI2909.1>
- Wang H, Chen Y, Pan Y, Li W (2015) Spatial and temporal variability of drought in the arid region of China and its relationships to teleconnection indices. *J Hydrol* 523:283–296. <https://doi.org/10.1016/j.jhydrol.2015.01.055>
- Wang H, Pan Y, Chen Y (2017) Comparison of three drought indices and their evolutionary characteristics in the arid region of northwestern China. *Atmos Sci Lett* 18:132–139. <https://doi.org/10.1002/asl.735>
- Wang Q, Liu Y, Zhang Y, Tong L, Li X, Li J, Sun Z (2019) Assessment of spatial agglomeration of agricultural drought disaster in China from 1978 to 2016. *Sci Rep-Uk* 9(1–8):3. <https://doi.org/10.1038/s41598-019-51042-x>
- Xu Y, Li Z, Wang L (2020) Temporal-spatial differences in and influencing factors of agricultural eco-efficiency in Shandong province, China. *Cienc Rural*. <https://doi.org/10.1590/0103-8478cr20190818>
- Yan H, Wang S, Wang J, Lu H, Guo A, Zhu Z, Myneni R, Shugart H (2016) Assessing spatiotemporal variation of drought in China and its impact on agriculture during 1982–2011 by using PDSI indices and agriculture drought survey data. *J Geophys Res Atmos* 121:2283–2298. <https://doi.org/10.1002/2015JD024285>
- Yang P, Huang X, Peng L, Zheng Z, Wu X, Xing C (2021) Safety evaluation of major hazard installations based on regional disaster system theory. *J Loss Prevent Proc* 69:104346. <https://doi.org/10.1016/j.jlp.2020.104346>
- Yang W, Zhang L, Gao Y (2022) Agricultural drought disaster characteristics and return period analysis in three Northeastern provinces. *J Arid Land Res Environ* 36(10):133–141
- Yang W, Zhang L, Yang Z (2023) Spatiotemporal characteristics of droughts and floods in Shandong Province, China and their relationship with food loss. *Chin Geogr Sci* 33:304–319. <https://doi.org/10.1007/s11769-023-1338-0>
- Yao T, Zhao Q, Li X, Shen Z, Ran P, Wu W (2021) Spatiotemporal variations of multi-scale drought in Shandong Province from 1961 to 2017. *Water Supply* 21(2):525–541. <https://doi.org/10.2166/ws.2020.332>
- Yevjevich V (1967) Objective approach to definitions and investigations of continental hydrologic droughts. An. Ph.D. thesis. Colorado State University. Libraries.
- Yi F, Li C, Feng Y (2018) Two precautions of entropy-weighting model in drought-risk assessment. *Nat Hazards* 93:339–347. <https://doi.org/10.1007/s11069-018-3303-2>
- Zarei A, Moghimi M, Koohi E (2021) Sensitivity assessment to the occurrence of different types of droughts using GIS and AHP techniques. *Water Resour Manag* 35:3593–3615. <https://doi.org/10.1007/s11269-021-02906-3>
- Zeng Z, Wu W, Li Z, Zhou Y, Guo Y, Huang H (2019) Agricultural drought risk assessment in southwest China. *Water* 11:1064. <https://doi.org/10.3390/w11051064>
- Zhang Z, Zhang Y, Sun Z, Zheng J, Liu E, Feng L, Feng C, Si P, Bai W, Cai Q, Yang N, Werf W, Zhang L (2019) Plastic film cover during the fallow season preceding sowing increases yield and water use efficiency of rain-fed spring maize in a semi-arid climate. *Agric Water Manage* 212:203–210. <https://doi.org/10.1016/j.agwat.2018.09.001>
- Zhang L, Wang Y, Chen Y, Bai Y, Zhang Q (2020a) Drought risk assessment in central Asia using a probabilistic copula function approach. *Water* 12:421. <https://doi.org/10.3390/w12020421>
- Zhang Q, Yao Y, Li Y, Huang J, Ma Z, Wang Z, Wang S, Wang Y, Zhang Y (2020b) Causes and changes of drought in China: research progress and prospects. *J Meteorol Res* 34:460–481. <https://doi.org/10.1007/s13351-020-9829-8>
- Zhang L, Liang C, Li T, Yang W (2022) A two-stage EDM method based on KU-CBR with the incomplete linguistic intuitionistic fuzzy preference relations. *Comput Ind Eng* 172:108552. <https://doi.org/10.1016/j.cie.2022.108552>
- Zhao Y, Yang N, Wei Y, Hu B, Cao Q, Tong K, Liang Y (2019) Eight hundred years of drought and flood disasters and precipitation sequence reconstruction in Wuzhou city, southwest China. *Water* 11:219. <https://doi.org/10.3390/w11020219>
- Zhou X, Wang P, Tansey K, Zhang S, Li H, Wang L (2020) Developing a fused vegetation temperature condition index for drought monitoring at field scales using sentinel-2 and Modis imagery. *Comput Electron Agric* 168:105144. <https://doi.org/10.1016/j.compag.2019.105144>

- Zhu X, Xu K, Liu Y, Guo R, Chen L (2021) Assessing the vulnerability and risk of maize to drought in China based on the Aquacrop model. *Agric Syst* 189:103040. <https://doi.org/10.1016/j.agsy.2020.103040>
- Zuo D, Cai S, Xu Z, Li F, Sun W, Yang X, Kan G, Liu P (2018) Spatiotemporal patterns of drought at various time scales in Shandong province of eastern China. *Theor Appl Climatol* 131:271–284. <https://doi.org/10.1007/s00704-016-1969-5>

Publisher's Note Springer Nature remains neutral with regard to jurisdictional claims in published maps and institutional affiliations.

Springer Nature or its licensor (e.g. a society or other partner) holds exclusive rights to this article under a publishing agreement with the author(s) or other rightsholder(s); author self-archiving of the accepted manuscript version of this article is solely governed by the terms of such publishing agreement and applicable law.